Charge-carrier density and interplane coupling in $Y_2Ba_4Cu_7O_{15}$: A Cu NMR-NQR study

R. Stern,* M. Mali, I. Mangelschots,† J. Roos, and D. Brinkmann
Physik-Institut, Universität Zürich, CH-8057 Zürich, Switzerland

J.-Y. Genoud, T. Graf, and J. Muller
Département de Physique de la Matière Condensée, Université de Genève, CH-1211 Genève, Switzerland

(Received 30 November 1993)

We report an observation of the ^{63,65}Cu nuclear quadrupole resonance (NQR) and nuclear magnetic resonance (NMR) in $Y_2Ba_4Cu_7O_{15}$. We have measured the temperature dependence of the Cu NQR frequency and spin-lattice relaxation at all four chemically inequivalent Cu sites, and of the Cu magnetic shift at two inequivalent plane Cu sites (for the magnetic field parallel and perpendicular to the **c** axis). The $Y_2Ba_4Cu_7O_{15}$ compound turns out to be a structure containing two inequivalent CuO_2 planes of differing doping levels, a multilattice in which $YBa_2Cu_4O_8$ blocks and $YBa_2Cu_3O_7$ blocks alternate. In the normal conducting state both the static and the dynamic electron spin susceptibilities of the individual planes of a double plane are governed by the *same* temperature dependence, which shows a behavior typical for an underdoped high-T_c compound. The same temperature dependence means strong coupling between these planes, with the lower limit of the coupling constant not much less than 30 meV. Although the planes are strongly coupled, their spin susceptibilities retain a distinct q dependence. The temperature variation of relaxation rate and Knight shift is described in terms of spin-gap formation or, alternatively, of frustrated phase separation. Below T_c, the common temperature dependence is lost, which could arise from the opening of two superconducting gaps that differ in the individual planes.

I. INTRODUCTION

The understanding of the electron spin correlations and their possible interplay with superconductivity in the complex high-T_c copper oxides have attracted considerable interest, since both aspects are of great importance for an adequate description of these materials. Over the last several years the nuclear magnetic resonance (NMR) and nuclear quadrupole resonance (NQR) have played a vital and significant role in the study of the low-frequency spectrum of the spin fluctuations by probing the wave-vector (q) and frequency (ω) dependent spin susceptibility, $\chi(q,\omega)$. Relevant information can be gained from the temperature dependence of both the magnetic shift tensor, and the nuclear spin-lattice relaxation rate at different atomic sites.[1–3]

Of special interest and importance are, among others, the CuO_2 double planes, that characterize a whole class of high-T_c compounds. Each of these double planes consists of a pair of closely spaced adjacent CuO_2 planes which are present in almost all high-T_c superconductors and where the superconductivity takes place.[4]

From the high-T_c compounds having CuO_2 double planes, the most intensively studied so far is $YBa_2Cu_3O_7$ for which now NMR-NQR data are available for all sites in the crystal structure.[1] Many of our NMR and NQR investigations[5–10] have focused on another double-plane structure, namely the $YBa_2Cu_4O_8$ compound[11] that is distinguished by its high thermal stability and precise stoichiometry which leads to well-defined samples with respect to their oxygen content. Their structural homogeneity is reflected by very narrow ^{63,65}Cu NQR lines.[5] The lower T_c of the $YBa_2Cu_4O_8$ compound, 82 K, compared to that of $YBa_2Cu_3O_7$, 92 K, can be qualitatively accounted for by its lower doping level. The main difference in the crystallographic structure of $YBa_2Cu_3O_7$ and $YBa_2Cu_4O_8$ is the double CuO chain in the latter.

Here we report in detail NQR and NMR measurements in the compound $Y_2Ba_4Cu_7O_{15}$,[10,3,12] which can be considered as a natural multilattice (Fig. 1), consisting of alternating $YBa_2Cu_4O_8$ (1-2-4 for short) and $YBa_2Cu_3O_7$ (1-2-3) blocks containing double and single CuO chains, respectively.[13] The $Y_2Ba_4Cu_7O_{15}$ compound has been synthesized under high-O_2 pressure by Karpinski and Kaldis.[14] However, single-phase samples can also be obtained under normal O_2 pressure.[15] By changing the oxygen content, T_c can be varied between 14 K and 95 K,[16,17] which is the highest T_c reached so far in the $Y_2Ba_4Cu_{6+n}O_{14+n}$ family. Thus, one of the fundamental questions concerning this compound is why its T_c is larger than the T_c of the parent compounds.

Our results reveal, among others, the existence of a strong coupling between the adjacent CuO_2 planes of *one double plane*. Such a coupling was found previously in $YBa_2Cu_3O_6$,[18] $YBa_2Cu_3O_{6.6}$,[19] and $YBa_2Cu_3O_7$ (Ref. 20) by neutron scattering experiments. In addition, we conclude that the alternating blocks are doped at different levels.

0163-1829/94/50(1)/426(12)/$06.00

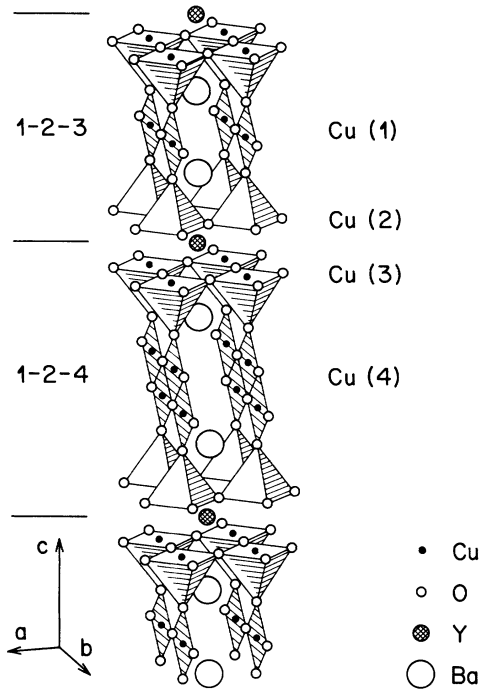

FIG. 1. Crystal structure of $Y_2Ba_4Cu_7O_{15}$ (Ref. 13). The upper two blocks represent one-half of the unit cell along the **c** axis. The crystal structure contains alternating 1-2-3 and 1-2-4 blocks.

The unit cell of $Y_2Ba_4Cu_7O_{15}$ contains *four* chemically inequivalent Cu sites: the Cu(1) chain and the Cu(2) plane sites of the 1-2-3 block and the Cu(3) plane and the Cu(4) chain sites of the 1-2-4 block. As in the $YBa_2Cu_3O_7$ and $YBa_2Cu_4O_8$ compounds, the CuO_2 planes in $Y_2Ba_4Cu_7O_{15}$ form double planes separated by Y ions. However, due to the alternation of 1-2-4 and 1-2-3 blocks, the double planes in $Y_2Ba_4Cu_7O_{15}$ consist of two *inequivalent* CuO_2 planes thus allowing one to study the coupling between such planes.

The lattice constants a and b nearly do not change upon going from $YBa_2Cu_4O_8$ to $Y_2Ba_4Cu_7O_{15}$, thus suggesting that the rigid 1-2-4 block determines the basal lattice constants of $Y_2Ba_4Cu_7O_{15}$. This suggestion is supported by the fact that the a, b, and c constants of $Y_2Ba_4Cu_7O_{15}$, in contrast to those of $YBa_2Cu_3O_7$, only slightly depend on the oxygen content. This might also be responsible for the oxygen disorder in the single chains of the 1-2-3 block. Neutron experiments for oxygen deficient samples[21] revealed that a certain number of single chains are lying in the a direction which is perpendicular to the double chains. However, for the high-oxygen content sample, as reported here, there is no misorientation in the single chain.[17]

The rest of the paper is organized as follows. The next section contains the necessary theoretical NMR-NQR background. Experimental procedures, including the characterization of the sample, are given in Sec. III. In Sec. IV we present our data, in Sec. V we discuss our results and compare them with neutron diffraction data and theoretical models. The paper concludes with a summary in Sec. VI.

II. NMR-NQR THEORY

A nuclear spin interacts with its electronic environment through electric and magnetic hyperfine couplings.[22] In the presence of an applied magnetic field, $\mathbf{B}_0$, the Hamiltonian of a nuclear spin, $\mathbf{I}$, having a quadrupole moment, eQ, can be written as

$$\mathcal{H} = \mathcal{H}_{\text{Zeeman}} + \mathcal{H}_{\text{quadrupole}} + \mathcal{H}_{\text{hyperfine}} \tag{1}$$

with

$$\mathcal{H}_{\text{Zeeman}} = -\gamma_n \hbar B_0 [I_z \cos\theta + I_y \sin\theta \sin\phi + I_x \sin\theta \cos\phi] , \tag{2}$$

$$\mathcal{H}_{\text{quadrupole}} = \frac{eQV_{zz}}{4I(2I-1)} \left(3I_z^2 - I(I+1) + \frac{\eta}{2}(I_+^2 + I_-^2) \right) , \tag{3}$$

and

$$\mathcal{H}_{\text{hyperfine}} = \gamma_n \hbar \left(\sum_j \mathbf{I} \cdot \mathbf{A}_j \cdot \mathbf{S}_j + \mathbf{I} \cdot \mathbf{O} \cdot \mathbf{L} \right) . \tag{4}$$

Here, $V_{\alpha\alpha}$ ($\alpha = x, y, z$) denote the principal components of the electric field gradient (EFG) tensor $\mathbf{V}$, with the axes labeled according to the convention $|V_{xx}| \leq |V_{yy}| \leq |V_{zz}|$. The asymmetry parameter of $\mathbf{V}$, η, is defined as $\eta = (V_{xx} - V_{yy})/V_{zz}$, $\eta \in [0,1]$. For a particular site, x, y, z are chosen as the frame of reference in Eqs. (1)–(4). In all Y-Ba-Cu-O compounds due to symmetry, one permutation of the x, y, z set coincides with the orthorhombic **a**, **b**, and **c** crystal axes. θ and ϕ are the polar and azimuth angles, respectively, of $\mathbf{B}_0$ in this crystal frame. $\mathbf{S}_j$ is the electron spin operator at the copper site j and $\mathbf{A}_j$ is its spin hyperfine tensor, the sum over j includes only on-site copper and its first neighbors. $\mathbf{L}$ is the electron orbital angular momentum and $\mathbf{O}$ is its on-site orbital hyperfine tensor. γ_n is the nuclear gyromagnetic ratio.

In the absence of an applied or an internal static magnetic field, the remaining $\mathcal{H}_{\text{quadrupole}}$ gives rise to doubly degenerate energy levels between which NQR transitions can be induced. For copper, there exist two naturally occurring isotopes ^{63}Cu and ^{65}Cu both having spin $\frac{3}{2}$ and thus two doubly degenerate $\pm\frac{1}{2}$ and $\pm\frac{3}{2}$ energy levels. For each isotope, a transition between these levels yields a single NQR signal at frequency

$$^{63,65}\nu_Q = \frac{e\,{}^{63,65}Q\,V_{zz}}{2h} \sqrt{1 + \frac{1}{3}\eta^2} . \tag{5}$$

In the presence of a large external magnetic field, $\mathbf{B}_0$, $\mathcal{H}_{\text{quadrupole}}$ causes, for each isotope and each site, a splitting of the Cu NMR signal into a central line arising from the central transition, $(+\frac{1}{2}, -\frac{1}{2})$, and two satellite

lines due to the $(\pm\frac{1}{2},\mp\frac{3}{2})$ transitions. In addition, the $\mathcal{H}_{\text{hyperfine}}$ term causes a magnetic shift of each line.

We now briefly summarize some properties of the EFG and the magnetic shift tensor. The EFG tensor is a ground-state property of a crystal depending sensitively on the charge distribution in the material. In a semiempirical approach, one assumes that the tensor can be written as the sum of two terms, a *lattice* and a *valence* contribution:

$$V_{\alpha\alpha} = V_{\alpha\alpha}^{\text{lat}} + V_{\alpha\alpha}^{\text{val}} \ . \tag{6}$$

The first contribution arises from all charges outside the ion under consideration. Using the point-charge model, this term is given by

$$V_{ij}^{\text{lat}} = [1-\gamma_\infty] \sum_k q_k \left(\frac{3x_i^k x_j^k - \delta_{ij}|\vec{x}^k|^2}{|\vec{x}^k|^5} \right), \tag{7}$$

where γ_∞ is the Sternheimer antishielding factor (approximately 10 for copper nuclei), q_k and x_k are the charge and the position of the kth ion, respectively.

The second term in Eq. (6) arises from nonfilled shells of the subject ion. In case of Cu^{2+} ions and taking into account only holes in the Cu $3d$ orbitals, we can write[23]

$$\begin{aligned} V_{zz}^{\text{val}} = &-\tfrac{4}{7} e\langle r^{-3}\rangle_{3d} [n_{3d(x^2-y^2)} - n_{3d(3z^2-r^2)} \\ &+ n_{3d(xy)} - \tfrac{1}{2} n_{3d(xz)} + \tfrac{1}{2} n_{3d(yz)}] \ , \end{aligned} \tag{8}$$

where $n_{3d(x,y,z)}$ are the number of holes in different $3d$ orbitals.

Because, in Y-Ba-Cu-O compounds, the positively charged on-site holes predominantly reside on the d orbitals extending towards the negatively charged neighbor oxygen ions, the lattice and valence contributions in Eq. (6) have opposite sign.

The *magnetic* coupling between the nuclear spin and its electronic environment as expressed by the $\mathcal{H}_{\text{hyperfine}}$ Hamiltonian [Eq. (4)] can be viewed as a coupling of the nuclear spin with a time dependent local magnetic hyperfine field $\mathbf{H}_L$ generated by the electron spin and the electron orbital motion. The static part of $\mathbf{H}_L$ gives rise to a NMR line shift expressed by the *magnetic shift tensor* $\mathbf{K}$, whose components, in the x,y,z reference frame, can be decomposed in a spin and an orbital part:

$$K_{\alpha\alpha}(T) = K_{\alpha\alpha}^{\text{spin}}(T) + K_{\alpha\alpha}^{\text{orb}} \ . \tag{9}$$

The spin part of the magnetic shift is usually called the Knight shift. In the high-T_c compounds, $\mathbf{K}^{\text{orb}}$ is predominantly temperature independent, whereas the temperature dependent $\mathbf{K}^{\text{spin}}$ is expected to vanish in the superconducting state due to singlet spin pairing.

Each part of the $\mathbf{K}$ tensor can be expressed by the respective hyperfine interaction tensor and the static electronic susceptibility as

$$K_{\alpha\alpha}^{\text{spin}} = \frac{1}{g\mu_B} \sum_j (A_j)_{\alpha\alpha} (\chi_j)_{\alpha\alpha}, \tag{10}$$

$$K_{\alpha\alpha}^{\text{orb}} = \frac{1}{\mu_B} O_{\alpha\alpha} \chi_{\alpha\alpha}^{\text{orb}} \ . \tag{11}$$

The fluctuating part of $\mathbf{H}_L$ is the source of the nuclear spin-lattice relaxation. In the case of high-T_c compounds, the main contribution to the copper spin-lattice relaxation stems from the electron spin fluctuations. After Moriya,[24] this contribution is related to the imaginary part of the dynamical spin susceptibility, $\chi(q,\omega_0)$, and the "relaxation rate per temperature unit," $(T_1T)^{-1}$, is given by

$$\left(\frac{1}{T_1T}\right)_\alpha = \frac{\gamma_n^2 k_B}{2\mu_B^2} \sum_{q,\alpha'\neq\alpha} |A(q)_{\alpha'\alpha'}|^2 \frac{\chi''_{\alpha'\alpha'}(q,\omega_0)}{\omega_0}, \tag{12}$$

$$A(q)_{\alpha\alpha} = \sum_j A_{j,\alpha\alpha} \exp(i\mathbf{q}\cdot\mathbf{r}_j).$$

Here, ω_0 is the nuclear resonance frequency. α denotes the direction of quantization, i.e., the direction of V_{zz} in NQR and of $\mathbf{B}_0$ in NMR experiments, and α' is the direction perpendicular to α. $\mathbf{A}_j$ is the on-site ($\mathbf{r}_j = 0$) and the transferred ($\mathbf{r}_j \neq 0$) hyperfine coupling tensor for the nuclei under consideration. Thus, the "relaxation rate per temperature unit" provides information about the q averaged imaginary part of $\chi(q,\omega_0)$.

III. EXPERIMENT

The $Y_2Ba_4Cu_7O_{15}$ sample, investigated in this work, was prepared by the solid state reaction technique, which is described in detail elsewhere.[25] The sample was calcined twice in oxygen gas (O_2) at 20 bar pressure and at 1020 °C during 12 h (reground in between) and postannealed in 100 bar O_2 at 300 °C during 3 days. Different characterization techniques (x-ray diffraction and TEM) show a pure $Y_2Ba_4Cu_7O_{15}$ phase without impurity phases within a detection limit of less than 0.5% by volume. No $YBa_2Cu_3O_7$ or $YBa_2Cu_4O_8$ phase precipitates were found. The absolute oxygen content of the sample was estimated on the base of the annealing treatment and the determined lattice parameters.[25] Some data for our sample are listed in Table I.

In order to study the anisotropic properties of the $Y_2Ba_4Cu_7O_{15}$ compound, the Cu NMR experiments were carried out on a c-axis oriented powder. The magnetic orienting of the powder, described in Ref. 27, produced a sample with a high degree of c-axis alignment of

TABLE I. Parameters of $Y_2Ba_4Cu_7O_z$ sample used in this study.

Crystallographic data	
a (Å)	3.834
b (Å)	3.879
c (Å)	50.61
V (Å^3)	752.7
$2(b-a)/(b+a)$ (%)	1.17
Transition onset	
T_c (K)	92.8
Oxygen content	
z	15.1(1)

the grains whereas the a and b axes remained randomly distributed.

The ^{63,65}Cu NQR and NMR experiments were carried out using standard pulsed spectrometers. The resonance signals were obtained by a phase alternating add-subtract spin-echo technique similar to that one used in Ref. 28.

The NQR measurements were done in a zero magnetic field. The spectra were obtained by scanning the frequency in discrete steps and integrating the echo signal. The spin-lattice relaxation time T_1 was measured by NQR using the inversion-recovery pulse sequence.

The NMR experiments were performed in an external magnetic field, $\mathbf{B}_0$, of 9.03 T using Fourier transformation of the spin echo. In all our experiments we used very intensive radio frequency pulses with optimal pulse lengths of 1.5 μs or less.

IV. RESULTS AND ANALYSIS

A. NQR

The $Y_2Ba_4Cu_7O_{15}$ ^{63,65}Cu NQR spectrum at 100 K (Fig. 2) looks almost like the combined NQR spectra of the parent compounds $YBa_2Cu_3O_7$ (Ref. 29) and $YBa_2Cu_4O_8$.[5] Therefore, naturally, we assigned the four ^{63}Cu and ^{65}Cu isotope pairs in the $Y_2Ba_4Cu_7O_{15}$ NQR spectrum on grounds of their resemblance in frequency and shape with the ones in the parent compounds. The correctness of such a choice is supported by the very similar temperature behavior of corresponding lines in $Y_2Ba_4Cu_7O_{15}$ and the parent compounds (Fig. 3). However, at closer inspection one notices that in $Y_2Ba_4Cu_7O_{15}$ the frequency difference between the single- and double-chain Cu lines is somewhat smaller than observed for the parent compounds. The same effect but less pronounced is observed for the plane lines.

One notices further that the lines in the 1-2-4 block are almost as narrow as in $YBa_2Cu_4O_8$ which demon-

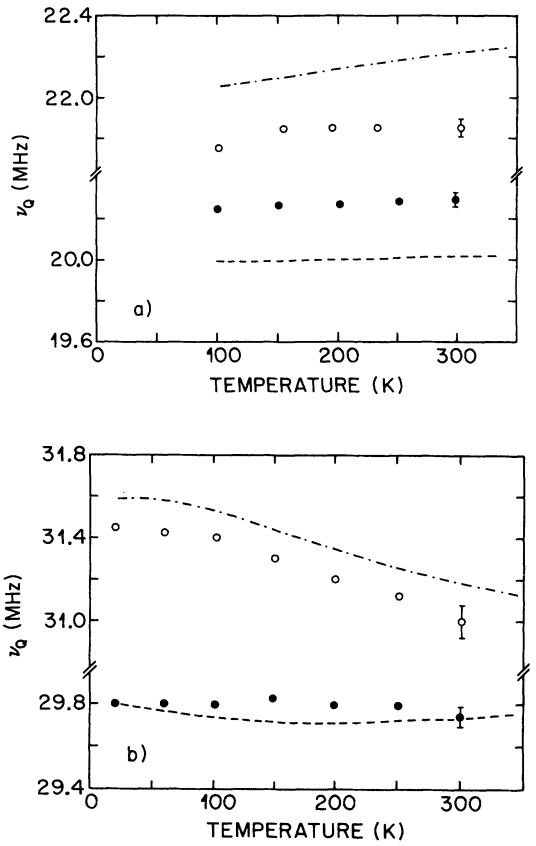

FIG. 3. Temperature dependence of the ^{63}Cu NQR frequency ν_Q. (a) At Cu(1) (open circles) and Cu(4) sites (filled circles) in $Y_2Ba_4Cu_7O_{15}$, compared to ν_Q at Cu(1) sites in $YBa_2Cu_3O_7$ (dash-dotted line, Ref. 29) and in $YBa_2Cu_4O_8$ (dashed line, Ref. 5). (b) At Cu(2) (open circles) and Cu(3) sites (filled circles) in $Y_2Ba_4Cu_7O_{15}$ compared to ν_Q at Cu(2) sites in $YBa_2Cu_3O_7$ (dash-dotted line, Ref. 29) and in $YBa_2Cu_4O_8$ (dashed line, Ref. 5).

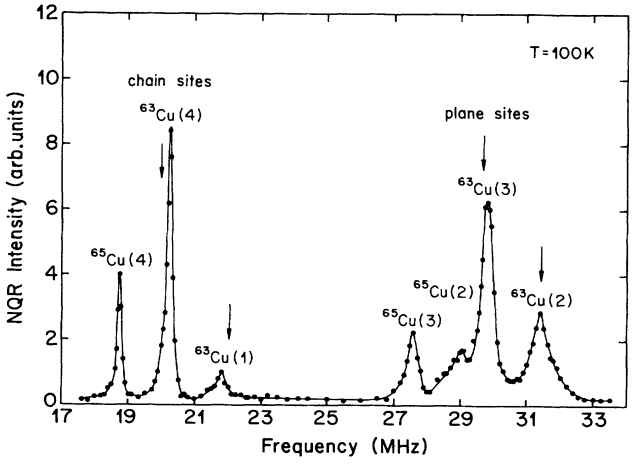

FIG. 2. The ^{63,65}Cu NQR spectrum in $Y_2Ba_4Cu_7O_{15}$ at 100 K. The points denote the integration of the spin echo over time. The intensities of the chain and plane lines are not to scale. The arrows denote the line positions in $YBa_2Cu_3O_7$ and $YBa_2Cu_4O_8$.

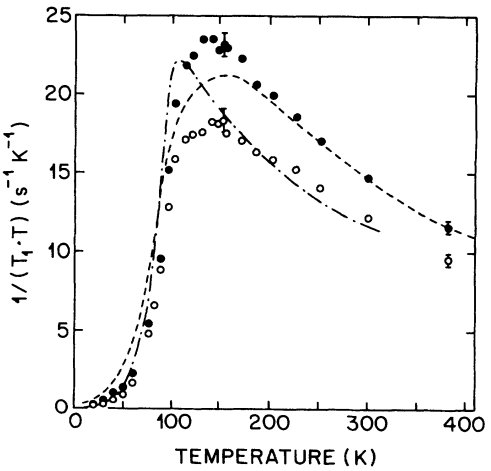

FIG. 4. Temperature dependence of ^{63}Cu $(T_1T)^{-1}$ measured by NQR at Cu(2) (open circles) and Cu(3) sites (filled circles) in $Y_2Ba_4Cu_7O_{15}$ compared to $(T_1T)^{-1}$ at Cu(2) sites in $YBa_2Cu_3O_7$ (dash-dotted line, Ref. 29) and in $YBa_2Cu_4O_8$ (dashed line, Ref. 5).

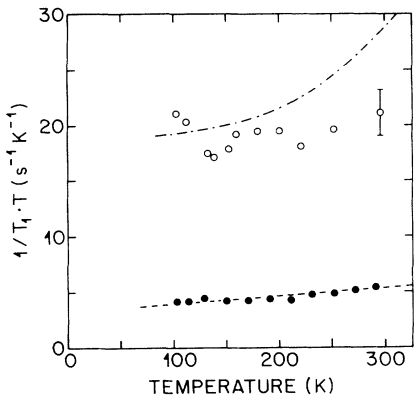

FIG. 5. Temperature dependence of ^{63}Cu $(T_1T)^{-1}$ measured by NQR at Cu(1) (open circles) and Cu(4) sites (filled circles) in $Y_2Ba_4Cu_7O_{15}$ compared to $(T_1T)^{-1}$ at Cu(1) in $YBa_2Cu_3O_7$ (dash-dotted line, Ref. 33) and in $YBa_2Cu_4O_8$ (dashed line, Ref. 5).

strates the structural quality of the 1-2-4 block being comparable to that of good $YBa_2Cu_4O_8$. In contrast, the chain and plane lines in the 1-2-3 block are much broader than corresponding lines in a good quality $YBa_2Cu_3O_7$ sample,[30] thus indicating that also in $Y_2Ba_4Cu_7O_{15}$ the single chain is an imperfect structural element which only under very subtle thermodynamic conditions can be ordered and filled completely with oxygen.

The spin-lattice relaxation rate has been measured by NQR for all four copper sites of $Y_2Ba_4Cu_7O_{15}$. Figure 4 depicts the temperature dependence of $(T_1T)^{-1}$ of Cu(2) and Cu(3) together with related data from $YBa_2Cu_3O_7$ (Ref. 31) and $YBa_2Cu_4O_8$.[6] Characteristic for $Y_2Ba_4Cu_7O_{15}$ is that $(T_1T)^{-1}$ for both planar sites depends strongly on temperature in the normal conducting state showing a maximum at $T^* = 130$ K combined with a Curie-Weiss-type behavior above and a strong drop below T^*.

The temperature dependence of $(T_1T)^{-1}$ for the chain Cu sites is given in Fig. 5. The Cu(4) data are practically identical with the corresponding values in $YBa_2Cu_4O_8$, thus demonstrating that the electronic spin dynamics of the double chains is unaffected by the $Y_2Ba_4Cu_7O_{15}$ multilattice and therefore remains equal in both compounds. For the Cu(1) data, the agreement with the $YBa_2Cu_3O_7$ data is less pronounced, partly due to the large scatter of the $Y_2Ba_4Cu_7O_{15}$ data. However, above 250 K, the two data sets clearly depart from each other.

B. NMR

Figure 6 shows the central lines of the Cu NMR spectrum obtained for two orientations of the magnetic field, $\mathbf{B}_0 \parallel \mathbf{c}$ and $\mathbf{B}_0 \perp \mathbf{c}$. The lines are shifted with respect to the Larmor frequency, ν_L, due to quadrupolar and magnetic hyperfine couplings. The quadrupolar as well as the magnetic shift depend on $\mathbf{B}_0$ but in a rather opposite manner: the magnetic shift is proportional to $\mathbf{B}_0$, the quadrupolar is proportional to $\mathbf{B}_0^{-1}$. Since we are mainly interested in the magnetic shifts, the spectrum was measured in a high magnetic field [$\nu_L(^{63}\text{Cu}) = 101.916$ MHz in CuCl].

In order to determine the **K** values from the asymmetrically broadened experimental multicentral-line spectra we used a line shape model that involves a convolution of a temperature independent Gaussian angular distribution of **c**-axis misalignment, responsible for an asymmetric second-order quadrupolar shift broadening of the resonance lines towards lower frequencies,[32] with a temperature dependent Lorentzian-like broadening present at each existing orientation. By varying the spread of the angular misalignment we achieved the best fit with a quite narrow Gaussian distribution width of only $\sim 2.5°$.

Because of Eq. (5) with ν_Q known from our NQR measurements, the analysis of the shift does not allow an unambiguous determination of eQV_{ZZ}, η, and **K**. However, it is known from previous studies[31,48] that the EFG at the plane Cu sites in $YBa_2Cu_3O_7$ as well as in $YBa_2Cu_4O_8$ is nearly axially symmetric with η values which are equal within the error limits (Table II). We assume that the

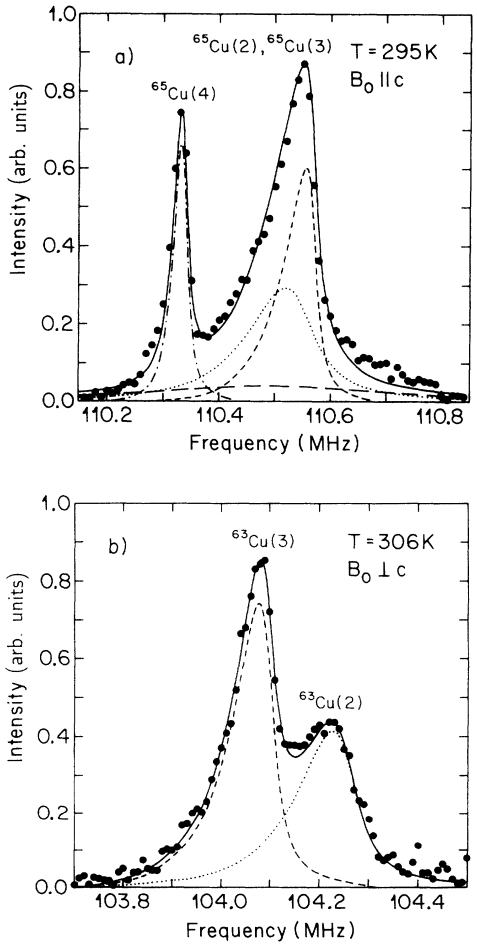

FIG. 6. The experimental (bullets) and calculated central lines of the Cu NMR spectrum for two orientations of the applied magnetic field. (a) $\mathbf{B}_0 \parallel \mathbf{c}$. ^{65}Cu(1): long-dashed, ^{65}Cu(2): dotted, ^{65}Cu(3): dashed, and ^{65}Cu(4): dash-dotted. (b) $\mathbf{B}_0 \perp \mathbf{c}$. ^{63}Cu(2): dotted and ^{63}Cu(3): dashed. The solid line is the sum of calculated individual lines.

TABLE II. The measured ^{63}Cu NQR frequences (ν_Q), linewidths (full width at half height), and asymmetry parameters (η) for various Y-Ba-Cu-O compounds at 100 K.

		ν_Q (MHz)	FWHH (kHz)	η	Ref.
$YBa_2Cu_3O_6$	Cu(1)	30.07(2)	140	0	26
	Cu(2)	23.8(2)[a]	70[a,b]	0	27
$YBa_2Cu_4O_8$	Cu(1)	20.00(3)	100(10)	0.951(5)[c]	6
	Cu(2)	29.74(6)	180(10)	0.015(5)[c]	6
$YBa_2Cu_3O_7$	Cu(1)	22.06(1)	90	0.984(5)[d]	29
	Cu(2)	31.53(1)	200	0.012(5)[d]	29
$Y_2Ba_4Cu_7O_{15}$	Cu(1)	21.80(5)	450(50)		This work
	Cu(2)	31.40(8)	750(50)		This work
	Cu(3)	29.80(5)	430(30)		This work
	Cu(4)	20.35(4)	180(30)		This work

[a]These values are obtained from NMR measurements of the paramagnetic phase in 5.17 T at 505 K.
[b]For the orientation $\mathbf{B_0} \parallel \mathbf{c}$.
[c]Reference 48.
[d]Reference 31.

η values at the Cu(2) and Cu(3) sites in $Y_2Ba_4Cu_7O_{15}$ are the same as the respective values in $YBa_2Cu_3O_7$ and $YBa_2Cu_4O_8$. This assumption, however, as long not verified, bears an uncertainty in the quadrupolar and consequently in the magnetic shift. To estimate the magnitude of a possible error, we evaluated $\mathbf{K}$ from the experimental spectrum for a variety of η's. The influence of η on $\mathbf{K}$ is quite modest insofar as η remains below 0.05, i.e., in the range of values typically observed at plane copper sites. The influence of η depends on the orientation of $\mathbf{B_0}$.

Measurements of plane Cu K_{cc} ($\mathbf{B_0} \parallel \mathbf{c}$) at room temperature were performed on the central transition of the less abundant ^{65}Cu isotope to avoid overlap of the plane Cu(2) and Cu(3) lines with the double-chain Cu(4) line.

The assignment of the various Cu lines in the experimental spectrum [Fig. 6(a)] was facilitated by the appreciable difference in spin-spin relaxation times between chain and plane Cu sites, as known from NQR. The most narrow (20 kHz) and the broadest ($\sim$ 500 kHz) lines in the $\mathbf{B_0} \parallel \mathbf{c}$ spectrum belong to the double-chain site ^{65}Cu(4) and the single-chain site ^{65}Cu(1), respectively. The remaining 105 kHz broad line we assigned to a composition of two plane ^{65}Cu(2) and ^{65}Cu(3) lines with slightly different K_{cc} shifts 1.26% and 1.28%, respectively. Even at 11.7 T these two lines could not be resolved. Thus, K_{cc} is *practically equal* for the two plane copper sites.

In the case of $\mathbf{B_0} \perp \mathbf{c}$, the plane Cu central lines of the more abundant ^{63}Cu isotope spectrum are far apart from the chain Cu lines, therefore preferentially this spectrum was used in the K_{aa} shift determination. As one can see in Fig. 6(b), the two ^{63}Cu(2) and ^{63}Cu(3) central lines are quite well resolved at room temperature. Unfortunately, with decreasing temperature due to the broadening and smaller frequency separation this resolution deteriorates. Taking into account the experimentally determined temperature variation of ν_Q's shown in Fig. 3 and by using the line shape model for $\mathbf{B_0} \perp \mathbf{c}$ orientation, we were able to extract the temperature dependence of the total K_{aa} ($= K_{bb}$) shifts for Cu(2) and Cu(3). However, to obtain the more relevant temperature dependent spin part $\mathbf{K^{spin}}$ one has to know the constant orbital part $\mathbf{K^{orb}}$, usually obtained as the rest $\mathbf{K}$ shift at temperatures far below T_c. In the case of $Y_2Ba_4Cu_7O_{15}$, as already mentioned, the broadening and the overlap of the two lines prevent an accurate enough determination of $\mathbf{K^{orb}}$. Therefore we had to resort on the values obtained by Barrett *et al.* for $YBa_2Cu_3O_7$ (Ref. 33) and by Zimmermann *et al.* for $YBa_2Cu_4O_8$.[6] As one may expect both values agree in er-

TABLE III. Room temperature ^{63}Cu shift data for plane sites of $YBa_2Cu_3O_7$ (Ref. 34), $YBa_2Cu_4O_8$ (Ref. 6), and $Y_2Ba_4Cu_7O_{15}$, in percent.

		K_{aa}^{orb}	K_{aa}^{spin}	K_{cc}^{orb}	K_{cc}^{spin}
$YBa_2Cu_3O_7$	Cu(2)	0.280	0.293	1.28	-0.01
$YBa_2Cu_4O_8$	Cu(2)	0.29(3)	0.23(3)	1.31(3)	0.00(3)
$Y_2Ba_4Cu_7O_{15}$	Cu(2)	0.285(20)	0.27(1)	1.26(2)	0.00(2)
	Cu(3)	0.285(20)	0.24(1)	1.28(2)	0.00(2)

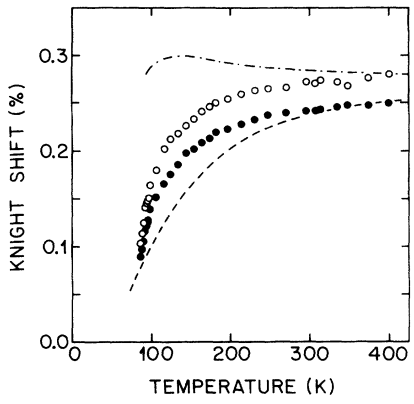

FIG. 7. Temperature dependence of the plane ^{63}Cu Knight shift at Cu(2) (open circles) and Cu(3) sites (filled circles) in $Y_2Ba_4Cu_7O_{15}$ compared to the Knight shift at Cu(2) sites in $YBa_2Cu_3O_7$ (dash-dotted line, Ref. 34) and in $YBa_2Cu_4O_8$ (dashed line, Ref. 6). The external field $\mathbf{B}_0$ lies perpendicular to the crystal c axis.

ror limits. Thus we took the average value of 0.285% for $K_{aa}^{\rm orb}(=K_{bb}^{\rm orb})$ of Cu(2) and Cu(3) (Table III). Subtraction of $K_{aa}^{\rm orb}$ from the respective total K_{aa} then yields the temperature dependent $K_{aa}^{\rm spin}$ for Cu(2) and Cu(3) (Fig. 7).

V. DISCUSSION

In this section we first discuss the two major topics of our study, the doping of the CuO_2 planes and the interplane coupling in $Y_2Ba_4Cu_7O_{15}$, and, then, analyze our data in terms of two phenomenological models providing analytical expressions for relaxation and Knight shift which can be readily evaluated.

A. Charge-carrier density in the CuO_2 planes

The EFG tensor [Eq. (8)] and hence ν_Q [Eq. (5)] of the plane copper sites is very sensitive to changes in the density of mobile holes, n, in the CuO_2 planes. Indeed, the NQR experiments in $YBa_2Cu_3O_{7-\delta}$ (Refs. 35 and 36) and $La_{2-x}Sr_xCuO_4$ (Ref. 37) show that ν_Q of the plane copper nuclei shifts towards higher values with increasing n. In the $YBa_2Cu_3O_{7-\delta}$ family, ν_Q changes from 23.18 MHz in undoped $YBa_2Cu_3O_6$ (Ref. 38) to 31.53 MHz at 100 K in $YBa_2Cu_3O_7$.[29] Optimal doping maximizing T_c occurs for $\delta = 0.06$.[39] In this sense, $YBa_2Cu_3O_7$ is overdoped and $YBa_2Cu_4O_8$ is underdoped. In the $La_{2-x}Sr_xCuO_4$ system, ν_Q increases linearly with Sr doping from 33 MHz for $x = 0$ to 36.2 MHz for $x = 0.15$.

The structural differences between various Y-Ba-Cu-O family members occur only in the CuO chains, leaving the nearest neighborhood of the plane Cu practically unchanged. The effects of these structural changes can be seen best of all via the NQR frequency of the Ba nuclei, ν_Q(Ba). Due to the closed electron shell of the Ba ion, ν_Q(Ba) is exclusively determined by the *lattice* contribution to the EFG and is as such very sensitive to structural changes. While ν_Q(Ba) in $YBa_2Cu_3O_7$ is still 6% higher than ν_Q(Ba) in $YBa_2Cu_4O_8$,[10] the ν_Q(Ba) of these parent substances differ only by 2% from the ν_Q(Ba) of the respective blocks in $Y_2Ba_4Cu_7O_{15}$.[40] Therefore it is reasonable to assume that the changes of the EFG and thus ν_Q of plane Cu in $YBa_2Cu_3O_7$, $YBa_2Cu_4O_8$, and $Y_2Ba_4Cu_7O_{15}$ arise predominantly from the changes of the EFG due to different in-plane dopings.

Based on these facts we can estimate n, the hole concentration per plane Cu atom, for the CuO_2 planes in the 1-2-3 and 1-2-4 blocks, respectively. In analogy to the $La_{2-x}Sr_xCuO_4$ system, we assume that ν_Q of the planar Cu in the Y-Ba-Cu-O compounds increases linearly with n, and use the ν_Q values of Table II (for 100 K). This way we find that n of the Cu(2)O_2 and Cu(3)O_2 planes in $Y_2Ba_4Cu_7O_{15}$ is 79 and 98%, respectively, of the hole concentration found in $YBa_2Cu_3O_7$, which means that the planes of the 1-2-3 block are more heavily doped than the planes of the 1-2-4 block. The doping levels do not change much with temperature since the variation of the corresponding ν_Q values with temperature is small.

To be quantitative, we calibrate the ν_Q-vs-n relation by assigning ν_Q of Cu(2) in undoped $YBa_2Cu_3O_6$ to $n = 0$ and by taking the formal 0.33 holes/Cu atom for $YBa_2Cu_3O_7$ as the n value corresponding to $\nu_Q = 31.53$ MHz. We thus obtain $d\nu_Q/dn = 23.4$ MHz/hole which compares well with the value 21 MHz/hole derived from $La_{2-x}Sr_xCuO_4$ data.[37] The 23.4 MHz/hole value then yields hole concentrations of 0.325 and 0.262 for the planes in the 1-2-3 and 1-2-4 blocks of $Y_2Ba_4Cu_7O_{15}$, respectively, and a concentration of 0.259 for $YBa_2Cu_4O_8$ planes. As suspected, the last two values are very close to the formal 0.25 holes/Cu atom in $YBa_2Cu_4O_8$.

The finding of different hole concentrations in the 1-2-3 and 1-2-4 blocks is qualitatively supported by plane Cu spin-lattice relaxation rate, W, and Knight shift data. It is now widely agreed that the relaxation at plane Cu sites is primarily caused by antiferromagnetic (AF) electron spin fluctuations which, according to neutron scattering experiments, get progressively suppressed by growing charge carrier density.[41] Hence, the room temperature relaxation rate in Y-Ba-Cu-O monotonically decreases with increasing CuO_2 plane doping.[42–44] Assuming that the same tendency holds for $Y_2Ba_4Cu_7O_{15}$, it follows from the Cu(2) and Cu(3) relaxation data that the 1-2-3 block has a higher doping level than the 1-2-4 block. Furthermore, at high temperature where the temperature dependence of W[Cu(2)] and W[Cu(3)] levels off, W[Cu(3)] agrees quite well with that of Cu(2) in $YBa_2Cu_4O_8$, indicating an equal charge carrier density in corresponding planes. The agreement of the Cu(2) relaxation rates in $YBa_2Cu_3O_7$ and in the 1-2-3 block is somewhat poorer. The slightly higher rate in the 1-2-3 block may be an indication of a somewhat lower doping level in this block.

In contrast to the relaxation rate, the Knight shift $K_{aa}^{\rm spin}$ in (Y,Pr)$Ba_2Cu_3O_7$,[44] $YBa_2Cu_3O_{7-\delta}$,[45] and in $Tl_2Ba_2CuO_{6+\delta}$ (Ref. 46) grows with increasing n. In $Y_2Ba_4Cu_7O_{15}$ the 1-2-3 block exhibits a larger shift than the 1-2-4 block (Fig. 7), which again supports the con-

clusion of a higher plane doping level in the 1-2-3 block as compared to the 1-2-4 block.

Summarizing the preceding findings, the multilattice compound $Y_2Ba_4Cu_7O_{15}$ turns out to be a structure containing *planes of differing doping level.* The planes in the 1-2-4 block (1-2-3 block) are slightly higher (lower) doped than those in the corresponding parent compounds.

B. Coupling of CuO_2 planes above T_c

In Figs. 4 and 7 we compare the temperature dependences of the relaxation rate, W, and of the spin part of the magnetic shift, K_{aa}^{spin}, measured in $Y_2Ba_4Cu_7O_{15}$ with corresponding values of $YBa_2Cu_3O_7$ and $YBa_2Cu_4O_8$. For both, W and K_{aa}^{spin}, the respective values coincide above 300 K, whereas in the range between T_c and 300 K the $Y_2Ba_4Cu_7O_{15}$ data show a temperature variation which appreciably differs from that observed for $YBa_2Cu_3O_7$ as well as $YBa_2Cu_4O_8$ data. The relaxation rates together with the Knight shifts of each plane of the double plane exhibit a temperature dependence typical for an underdoped high-T_c superconductor. Furthermore, as evident from Fig. 8, in the normal conducting state at temperatures above 100 K, a constant relaxation rate ratio $r_W = W[\mathrm{Cu(3)}]/W[\mathrm{Cu(2)}] = 1.28(7)$ together with a constant shift ratio $r_K = K_{aa}^{spin}[\mathrm{Cu(3)}]/K_{aa}^{spin}[\mathrm{Cu(2)}] = 0.90(6)$ are observed.

According to Eq. (10) and Eq. (12), the temperature independent r_K and r_W imply a temperature independent relationship between the respective static and dynamic electronic spin susceptibilities. The relaxation rate, strictly speaking, involves the q averaged imaginary part of $\chi(q,\omega_0)$. However, if we assume that the spin fluctuations at the corner of the Brillioun zone, $q = Q_{AF}$, dominate the relaxation, the sum over q can be replaced by $\chi''(Q_{AF})$. The plane copper hyperfine constants appearing in the ratios are alike in Y-Ba-Cu-O compounds[47,48] and seem to be temperature independent. In other words, both the static and the dynamic

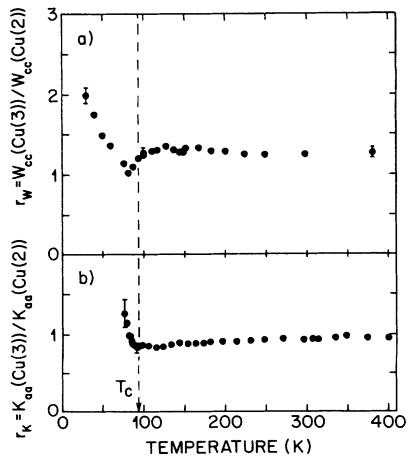

FIG. 8. Temperature dependence of the ratio of plane copper (a) relaxation rates and (b) Knight shifts in $Y_2Ba_4Cu_7O_{15}$.

electron susceptibilities of the two single planes of each double plane are governed by the *same* temperature dependence which means common spin dynamics in both planes, and hence these planes must be strongly coupled. However, since r_K and r_W are not equal, the q dependence of the susceptibility is not the same in the two planes.

A strong interplane coupling was recently observed by neutron scattering in the insulating antiferromagnetic $YBa_2Cu_3O_6$ (Ref. 18) and in superconducting $YBa_2Cu_3O_{6.6}$ (Ref. 19) and $YBa_2Cu_3O_7$.[20] In $YBa_2Cu_3O_6$, the large interplane exchange coupling (with coupling constant of about 15 meV) orders the next-nearest CuO_2 planes antiferromagnetically below the Néel temperature, T_N. In $YBa_2Cu_3O_{6.6}$ and in $YBa_2Cu_3O_7$ a similar interplane coupling produces strong AF electron spin-spin correlations which persist from the normal into the superconducting state. Note, however, that the coupled planes in these compounds are *equivalent* in contrast to those in $Y_2Ba_4Cu_7O_{15}$.

At the moment the mechanism of interplane coupling in $Y_2Ba_4Cu_7O_{15}$ is not known. Direct and indirect exchange interactions are possible candidates. Because of the relatively large interplane distance of 3.2 Å a direct exchange between the small Cu $3d_{3z^2-r^2}$ orbitals seems to be less likely and probably an indirect superexchange via oxygen and yttrium must be invoked. The coupling *strength* may be estimated from the K_{aa}^{spin}-vs-temperature plot (Fig. 7). Below 300 K, the K_{aa}^{spin} shifts in the 1-2-3 and 1-2-4 blocks begin to depart from those in $YBa_2Cu_3O_7$ and $YBa_2Cu_4O_8$ due to the interplane coupling, thus the coupling strength is not much less than $k_B \times 300$ K or 30 meV.

The strong AF interplane correlations observed in $YBa_2Cu_3O_{6.6}$ and in $YBa_2Cu_3O_7$ by neutron experiments are presumably present also in $Y_2Ba_4Cu_7O_{15}$. Then, as pointed out by Tranquada *et al.*,[19] the correlations impose restrictions on the charge-carrier movement which has to be of a special kind, most probably coherent in both planes to retain the interplane spin-spin correlations.

Irrespective of its nature, the question remains whether the interplane coupling favors or impedes superconductivity. Several theories of high-T_c superconductivity incorporate the interplane coupling as an essential ingredient. In the theory of Anderson,[49] only the interplane pair tunneling between coupled planes makes superconductivity possible. Altshuler and Ioffe[50] stress the importance of interplane correlations, arguing that they are essential for the system to become superconducting. The possibility of (nodeless) d-wave superconductivity in a double-plane model is predicted by Bulut *et al.*[51] and by Dagotto *et al.*[52] Morgenstern *et al.*[53] find evidence of d-wave superconductivity in their Monte Carlo simulations of the double-plane Hubbard model.

To our knowledge, none of the theories taking into account interplane coupling find it unfavorable for superconductivity. On the other hand, Eenige *et al.*[54] claim that the occurrence of superconductivity in $Y_2Ba_4Cu_7O_{15}$ is due to the proximity effect rather than to an interplane coupling. Their argument is based on a

kink seen in the pressure dependence of T_c. In order to explain a T_c being higher than in $YBa_2Cu_4O_8$ and even $YBa_2Cu_3O_7$, the authors, however, are forced to postulate an extra doping via interstitial oxygen.

Our experiments, however, clearly demonstrate the presence of an interplane coupling in $Y_2Ba_4Cu_7O_{15}$. Obviously, we cannot tell whether this coupling favors or impedes superconductivity. Nevertheless, our result fits into the framework of several theories favoring interplane coupling (see, for instance, Ref. 55).

A final comment concerns the high value of T_c. As pointed out in the preceding section, the 1-2-3 block in $Y_2Ba_4Cu_7O_{15}$ is close to or even at optimal doping for the $YBa_2Cu_3O_{7-\delta}$ structure. Thus it is tempting to assume that the "best plane," namely that of the 1-2-3 block, determines T_c. However, this argument fails for a composition of $Y_2Ba_4Cu_7O_{15}$ which yields a T_c of 95 K since, to our knowledge, the T_c values of $YBa_2Cu_3O_{7-\delta}$ do not exceed 93 K. Thus, it is conceivable that the interplane coupling plays a role in obtaining high-T_c values. NMR-NQR experiments on $Y_2Ba_4Cu_7O_{15}$ samples with $T_c = 95$ K may perhaps provide answers to this issue.

C. Interplane coupling below T_c

Next we will discuss briefly the relevance of the temperature dependence of W and K_{aa}^{spin} close and below T_c. Just above T_c, r_W begins to diminish with decreasing temperature. After smoothly passing into the superconducting state it decreases to a minimum of 1.0 at 80 K, where it starts to increase again. In contrast, r_K remains constant down to T_c, where it starts to increase. Unfortunately, the overlap of Cu(2) and Cu(3) lines prevents measurements of r_K below 76 K. Both ratios have the same value, namely 1.0, around 80 K which is close to T_c of $YBa_2Cu_4O_8$. Whether this is purely accidental remains an open question.

The variation of r_W and r_K with temperature in the superconducting state means that the susceptibilities of the individual planes of the double plane have lost their common temperature dependence. It is tempting to assume a weakening or even loss of the interplane coupling as the underlying cause. This, however, would contradict the results of neutron scattering experiments in $YBa_2Cu_3O_{6.6}$ (Ref. 19) and $YBa_2Cu_3O_7$,[20] where no significant change of the interplane correlation at and below T_c is observed. There is also evidence for strong coupling between the superconducting CuO_2 planes in $YBa_2Cu_3O_7$ from single-crystal transport measurements.[56]

Another reason why the common temperature dependence disappears could be a formation of two superconducting gaps that differ in the individual planes because of their different charge-carrier densities, n. However, up to now even the spatial symmetry of the superconducting state in Y-Ba-Cu-O and so the form of the superconducting gap is not well established, let alone its dependence on n. Thus, the explanation of the temperature variation of r_W and r_K below T_c is still missing.

D. Relaxation and Knight shift mechanisms

The crucial point in deriving the spin-lattice relaxation rate [Eq. (12)] and the Knight shift [Eq. (10)] is the calculation of the susceptibility, $\chi(q,\omega_0)$. In the absence of a complete understanding of the electronic state of Y-Ba-Cu-O superconductors, approximations must be introduced.

In the phenomenological model of Millis, Monien, and Pines (MMP),[57,3] $\chi(q,\omega_0)$ is treated in a mean-field approximation and it is decomposed into a quasiparticle (normal Fermi-liquid-like) contribution and a contribution arising from AF correlations. The MMP model gives a quantitative account of relaxation data at Cu, O, and Y sites in $YBa_2Cu_3O_7$ (Ref. 57) and at Cu(2) sites in $YBa_2Cu_4O_8$ (Ref. 10) provided the square of the correlation length of the AF fluctuations, ξ^2, has approximately a Curie-Weiss-like temperature dependence. Since neutron scattering investigations[18] concluded that ξ is temperature independent the applicability of the MMP model has been questioned.

A different approach to explain the anomalous temperature dependence of the relaxation rate has been suggested by Millis and Monien.[58] From their analysis of relaxation data, they concluded that the spectral weight in the spin fluctuations decreases as the temperature is lowered. This missing spectral weight must reappear at a higher energy in the form of a transition over a "spin pseudogap," Δ. Thus, there are two competing effects which determine the variation of T_1 with temperature: the increase of AF fluctuations with falling temperature and the spin-gap effect. At a certain temperature the spin-gap effect wins and $(T_1T)^{-1}$ starts to decrease. The widespread nature of the spin-gap effect has been noted by Rice.[59]

After the discovery of the spin-gap effect in $YBa_2Cu_3O_{7-\delta}$ by neutron scattering[60] several NMR groups have regarded the spin-gap effect to be responsible for the peculiar temperature variation of the relaxation rate, at least in the normal conducting state.[3] The relaxation rate is described by an *ad hoc* formula:

$$\frac{1}{T_1T} = \left(\frac{A_0}{T}\right)^{\alpha}\left[1-\tanh^2\left(\frac{\Delta_{\text{AF}}}{2T}\right)\right]. \tag{13}$$

Here, Δ_{AF} denotes the spin-gap energy at the $Q_{\text{AF}} = (\frac{\pi}{a},\frac{\pi}{a})$ since the Cu relaxation is dominated by the strong AF fluctuations around Q_{AF}.[57] A_0 is a constant and the factor $T^{-\alpha}$ guarantees a reasonable description for the high-temperature behavior and may be attributed to the gradual decay of AF correlations at higher temperatures.[57] Some applications of Eq. (13) to both Knight shift and relaxation rates are discussed in Refs. 61 and 62.

Figure 9 shows the fit of Eq. (13) to the Cu(2) and Cu(3) relaxation rates in $Y_2Ba_4Cu_7O_{15}$. The parameters for both fits are $\Delta_{\text{AF}} = 240(20)$ K and $\alpha = 1.25$ which within the error limits agree with $\Delta_{\text{AF}} = 260(10)$ K and $\alpha = 1.25$ we obtained for $YBa_2Cu_4O_8$ using our previous Cu(2) data.[6] This result again demonstrates the dominating role played by the double-chain block

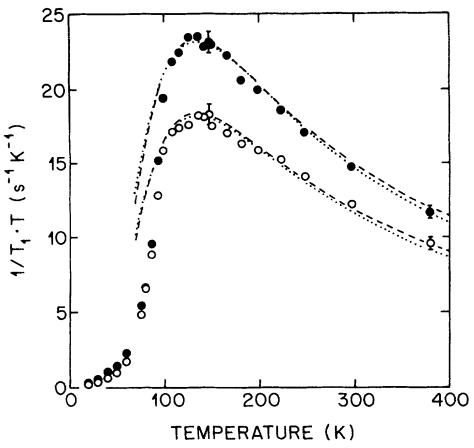

FIG. 9. The fits of Eq. (13) (dashed lines) and of Eq. (15) (dotted lines) to the measured Cu(2) (open circles) and Cu(3) (filled circles) relaxation rates in $Y_2Ba_4Cu_7O_{15}$. The parameters (for both sites) are $\Delta_{AF} = 240$ K and $\alpha = 1.25$ for Eq. (13) and $\omega_g = 250$ K for Eq. (15).

in $Y_2Ba_4Cu_7O_{15}$. A similar relaxation rate behavior of plane copper is observed for the bulk oxygen deficient $YBa_2Cu_3O_{7-\delta}$ ($\delta > 0.06$) material.[42]

The spin shift data are fitted by a similar *ad hoc* expression:

$$K_{aa}^{\text{spin}}(T) = K_0^{\text{spin}}\left[1 - \tanh^2\left(\frac{\Delta_0}{2T}\right)\right], \tag{14}$$

where Δ_0 is the spin-gap energy at $q = (0,0)$. Equation (14) describes quite well $K_{aa}^{\text{spin}}(T)$ in the normal conducting state. For $Y_2Ba_4Cu_7O_{15}$, the fit yields for both blocks a common $\Delta_0 = 150(20)$ K and two separate prefactors: $K_0^{\text{spin}} = 0.290\%$ for the 1-2-3 and $K_0^{\text{spin}} = 0.260\%$ for the 1-2-4 block. The same fit procedure applied to $YBa_2Cu_4O_8$ data yields $\Delta_0 = 210(20)$ K and $K_0^{\text{spin}} = 0.267\%$. Provided the temperature variation of the Knight shift arises from a spin-gap opening and Eq. (14) represents an appropriate description of this effect, then the results imply, first, that a spin gap, Δ_0, opens at $q = (0,0)$ and, second, that Δ_0 is smaller than Δ_{AF}.

We conclude this section by mentioning a completely different approach[63] to interpret the plane Cu relaxation rate. The high-T_c superconducting compound is viewed as a dilute system of neutral holes in an antiferromagnet that tends to separate into hole-rich and hole-poor phases, but is frustrated by long-range Coulomb interactions. As a consequence, large-amplitude local hole density fluctuations occur and their interaction with the mobile holes determines the normal conducting state properties. By approximating the fluctuations with a single-mode spin-1 excitation of wave vector Q_{AF} and energy ω_g, Emery and Kivelson[63] deduced for the relaxation rate the following expression:

$$\frac{1}{T_1T} = \frac{C_0}{T}\left[4 + \exp\left(\frac{\omega_g}{kT}\right) + 3\exp\left(-\frac{\omega_g}{kT}\right)\right]^{-1}, \tag{15}$$

where C_0 is a constant. As seen in Fig. 9, this formula allows quite a good fit to the plane Cu relaxation data, delivering $\omega_g = 250(10)$ K for $Y_2Ba_4Cu_7O_{15}$ and 270(10) K for $YBa_2Cu_4O_8$.

We like to stress that we have restricted our discussion of relaxation and Knight shift data to the previous two models only simply for the fact that Eqs. (13)–(15) contain parameters easely obtained by fitting the data. However, it is obvious that one cannot discriminate between these two models on the basis of our NMR experiments only.

VI. SUMMARY

We have reported the first observation of Cu NQR-NMR in $Y_2Ba_4Cu_7O_{15}$. In zero magnetic field we have measured the temperature dependence of the copper NQR frequency and spin-lattice relaxation at all four chemically inequivalent copper sites. In a 9.03 T magnetic field applied parallel and perpendicular to the **c** axis of an oriented powder sample, we have determined the temperature dependence of the copper magnetic shift at the two inequivalent plane copper sites.

The $Y_2Ba_4Cu_7O_{15}$ compound turns out to be a structure containing two inequivalent CuO_2 planes of differing doping levels. Thus, $Y_2Ba_4Cu_7O_{15}$ is the first double-plane cuprate where the interplane coupling could be accessed by Cu NMR-NQR studies.

In the normal conducting state, both the static and the dynamic electron spin susceptibilities of the individual planes of a double plane are governed by the *same* temperature dependence. This means a common spin dynamics in both planes, and hence these planes must be strongly coupled. The estimated lower limit of the corresponding interplane coupling is not much less than 30 meV. Although the planes are strongly coupled, their spin susceptibilities retain a distinct q dependence. The temperature dependence itself is typical for an underdoped high-T_c compound.

Below T_c, the common temperature dependence is lost, which could arise from the opening of two superconducting gaps that differ in the individual planes, thus manifesting the different plane charge carrier densities of the 1-2-4 and 1-2-3 blocks.

Two models were used to fit the experimental data in the normal conducting phase. The temperature variation of both the relaxation rate and the Knight shift at planar sites can be described as the effect of the opening of a spin gap yielding spin-gap values of 240 K and 150 K at wave vectors $Q_{AF} = (\frac{\pi}{a}, \frac{\pi}{a})$ and $q = (0,0)$, respectively. The corresponding values for $YBa_2Cu_4O_8$ are $\Delta_{AF} = 260$ K and $\Delta_0 = 210$ K.

Applying the "frustrated phase separation" model due to Emery and Kivelson to the planar Cu relaxation in

$Y_2Ba_4Cu_7O_{15}$ yields 250 K for the large-amplitude low-energy ω_g fluctuations of the local hole density. Since both models allow fits that remain well in the limits of the experimental error bars, a discrimination of these models on the basis of presently available experimental data is not possible.

ACKNOWLEDGMENTS

We thank Ivo Heinmaa for many useful discussions and for the NMR measurements at 11.7 T. Financial support by the Swiss National Science Foundation is gratefully acknowledged.

---

*Also at the Institute of Chemical Physics and Biophysics, EE-0001 Tallinn, Estonia.

†Present address: Laboratorium für Festkörperphysik, ETH–Hönggerberg, CH-8093 Zürich, Switzerland.

[1] C. H. Pennington and C. H. Slichter, in *Physical Properties of High Temperature Superconductors II* , edited by D. M. Ginsberg (World Scientific, New York, 1990).

[2] Appl. Magn. Reson. **3**, 383 (1992). A special issue containing contributions of NMR-NQR work in cuprate superconductors.

[3] D. Brinkmann and M. Mali, in *NMR - Basic Principles and Progress*, edited by P. Diehl, E. Fluck, H. Günther, R. Kosfeld, and J. Seelig (Springer, Berlin, 1994), Vol. 31, p. 171.

[4] P. W. Anderson, Science **256**, 1526 (1992).

[5] H. Zimmermann, M. Mali, D. Brinkmann, J. Karpinski, E. Kaldis, and S. Rusiecki, Physica C **159**, 681 (1989).

[6] H. Zimmermann, M. Mali, I. Mangelschots, J. Roos, L. Pauli, D. Brinkmann, J. Karpinski, S. Rusiecki, and E. Kaldis, J. Less-Common Met. **164-165**, 138 (1990).

[7] I. Mangelschots, M. Mali, J. Roos, D. Brinkmann, S. Rusiecki, J. Karpinski, and E. Kaldis, Physica C **194**, 277 (1992).

[8] M. Bankay, M. Mali, J. Roos, I. Mangelschots, and D. Brinkmann, Phys. Rev. B **46**, 11 228 (1992).

[9] D. Brinkmann, Z. Naturforsch. Teil A **47**, 1 (1992).

[10] I. Mangelschots, M. Mali, J. Roos, R. Stern, M. Bankay, A. Lombardi, and D. Brinkmann, in *Phase Separation in Cuprate Superconductors*, edited by K. A. Müller and G. Benedek (World Scientific, Singapore, 1993), p. 262.

[11] J. Karpinski, E. Kaldis, E. Jilek, S. Rusiecki, and B. Bucher, Nature **336**, 660 (1988).

[12] D. Brinkmann, Proceedings of the 2nd International Discussion Meeting on Relaxation in Complex Systems, Alicante, 1993 [J. Non-Cryst. Solids (to be published)].

[13] P. Bordet, C. Chaillout, J. Chenavas, J. Hodeau, M. Marezio, J. Karpinski, and E. Kaldis, Nature **334**, 596 (1988).

[14] J. Karpinski and E. Kaldis, Nature **331**, 242 (1988).

[15] K. Koyama, A. Junod, T. Graf, G. Triscone, and J. Muller, Physica C **185-189**, 461 (1991).

[16] J.-Y. Genoud, T. Graf, A. Junod, D. Sanchez, G. Triscone, and J. Muller, Physica C **177**, 315 (1991).

[17] H. Schwer, E. Kaldis, J. Karpinski, and C. Rossel, Physica C **211**, 165 (1993).

[18] J. Rossat-Mignod, L. P. Regnault, C. Vettier, P. Bourges, P. Burlet, J. Bossy, J. Y. Henry, and G. Lapertot, Physica B **180-181**, 383 (1992).

[19] J. M. Tranquada, P. M. Gehring, G. Shirane, S. Shamoto, and M. Sato, Phys. Rev. B **46**, 5561 (1992).

[20] H. A. Mook, M. Yethiraj, G. Aeppli, T. E. Mason, and T. Armstrong, Phys. Rev. Lett. **70**, 3490 (1993).

[21] A. W. Hewat, P. Fischer, E. Kaldis, E. A. Hewat, E. Jilek, J. Karpinski, and S. Rusiecki, J. Less-Common Met. **164-165**, 39 (1990).

[22] A. Abragam, *The Principles of Nuclear Magnetism* (Clarendon, Oxford, 1961).

[23] M. E. Garcia and K. H. Bennemann, Phys. Rev. B **40**, 8809 (1989).

[24] T. Moriya, J. Phys. Soc. Jpn. **18**, 516 (1963).

[25] J.-Y. Genoud, T. Graf, G. Triscone, A. Junod, and J. Muller, Physica C **192**, 137 (1992).

[26] K. Müller, M. Mali, J. Roos, and D. Brinkmann, Physica C **162-164**, 173 (1989).

[27] M. Mali, I. Mangelschots, H. Zimmermann, and D. Brinkmann, Physica C **175**, 581 (1991).

[28] C. H. Pennington, Ph.D. thesis, University of Illinois, 1989.

[29] M. Mali, D. Brinkmann, L. Pauli, J. Roos, H. Zimmermann, and J. Hulliger, Phys. Lett. A **124**, 112 (1987).

[30] H. Schiefer, M. Mali, J. Roos, H. Zimmermann, and D. Brinkmann, Physica C **162-164**, 173 (1989).

[31] C. H. Pennington, D. J. Durand, C. P. Slichter, J. P. Rice, E. D. Bukowski, and D. M. Ginsberg, Phys. Rev. B **39**, 2902 (1989).

[32] M. H. Cohen and F. Reif, Solid State Phys. **5**, 321 (1957).

[33] S. E. Barrett, D. J. Durand, C. H. Pennington, C. P. Slichter, T. A. Friedmann, J. P. Rice, and D. M. Ginsberg, Phys. Rev. B **41**, 6283 (1990).

[34] R. E. Walstedt, R. F. Bell, L. F. Schneemeyer, J. V. Waszczak, and G. P. Espinosa, Phys. Rev. B **45**, 8074 (1992).

[35] W. W. Warren, Jr., R. E. Walstedt, G. F. Brennert, P. J. Cava, B. Batlogg, and L. W. Rupp, Phys. Rev. B **39**, 831 (1989).

[36] I. Heinmaa, H. Lütgemeier, S. Pekker, G. Krabbes, and M. Buchgeister, Appl. Magn. Res. **3**, 689 (1992).

[37] T. Imai, C. P. Slichter, K. Yoshimura, and K. Kosuge, Phys. Rev. Lett. **70**, 1002 (1993).

[38] P. Mendels and H. Alloul, Physica C **156**, 355 (1988). This value is calculated via exact diagonalization of the Hamiltonian using zero field NMR data at 4.2 K. We assume that the frequency changes negligibly with temperature.

[39] T. Graf, G. Triscone, and J. Muller, J. Less-Common Met. **159**, 349 (1990).

[40] R. Stern (unpublished).

[41] G. Shirane, Physica C **185-189**, 80 (1991).

[42] C. Berthier, Y. Berthier, P. Butaud, W. G. Clark, J. A. Gillet, M. Horvatic, P. Ségransan, and J. Y. Henry, Appl. Magn. Res. **3**, 449 (1992).

[43] M. Takigawa, A. P. Reyes, P. C. Hammel, J. D. Thompson, R. F. Heffner, Z. Fisk, and K. C. Ott, Phys. Rev. B **43**, 247 (1991).

[44] A. P. Reyes, D. E. MacLaughlin, M. Takigawa, P. C. Hammel, R. H. Heffner, J. D. Thompson, and J. E. Crow, Phys. Rev. B **43**, 2989 (1991).

[45] T. Shimizu, H. Yasuoka, T. Tsuda, K. Koga, and Y. Ueda, Bull. Magn. Res. **12**, 39 (1990).

[46] Y. Kitaoka, K. Ishida, S. Ohsugi, K. Fujiwara, G.-q. Zheng,

and K. Asayama, Appl. Magn. Res. **3**, 549 (1992).
[47]T. Imai, J. Phys. Soc. Jpn. **59**, 2508 (1990).
[48]H. Zimmermann, Ph.D. thesis, University of Zurich, 1991.
[49]P. W. Anderson, in *Strong Correlation and Superconductivity*, edited by H. Fukuyama, S. Maekawa, and A. P. Malozemoff (Springer-Verlag, Berlin, 1989).
[50]P. L. Altshuler and L. B. Ioffe, Solid State Commun. **82**, 253 (1992).
[51]N. Bulut, D. J. Scalapino, and R. T. Scalettar, Phys. Rev. B **45**, 5577 (1992).
[52]E. Dagotto, J. Riera, and D. J. Scalapino, Phys. Rev. B **45**, 5744 (1992).
[53]I. Morgenstern, Th. Husslein, J. M. Singer, and H.-G. Matuttis, J. Phys. II (France) **2**, 1489 (1992).
[54]E. N. van Eenige, R. Griessen, K. Heeck, H. G. Schnack, R. J. Wijngaarden, J.-Y. Genoud, T. Graf, A. Junod, and J. Muller, Europhys. Lett. **20**, 41 (1992).
[55]A. J. Millis and H. Monien (unpublished); L. B. Ioffe, A. I. Larkin, A. J. Millis, and P. L. Altshuler (unpublished); M. U. Ubbens and P. A. Lee (unpublished).
[56]J. R. Rice, J. Giapintzakis, D. M. Ginsberg, and J. M. Mochel, Phys. Rev. B **44**, 10158 (1991).
[57]A. J. Millis, H. Monien, and D. Pines, Phys. Rev. B **42**, 167 (1990); H. Monien, D. Pines, and M. Takigawa, *ibid.* **43**, 258 (1991).
[58]A. J. Millis and H. Monien, Phys. Rev. B **45**, 3059 (1992).
[59]T. M. Rice, in *The Physics and Chemistry of Oxide Superconductors*, edited by Y. Iye (Springer-Verlag, Tokyo, 1992).
[60]J. Rossat-Mignod, L. P. Regnault, C. Vettier, P. Burlet, J. Y. Henry, and G. Lapertot, Physica B **169**, 58 (1991).
[61]M. Mehring, Appl. Magn. Res. **3**, 383 (1992).
[62]N. Winzek, Hj. Mattausch, S.-G. Eriksson, C. Ström, R. K. Kremer, A. Simon, and M. Mehring, Physica C **205**, 45 (1993).
[63]V. J. Emery and S. A. Kivelson, in *Phase Separation in Cuprate Superconductors*, edited by K. A. Müller and G. Benedek (World Scientific, Singapore, 1993).